Neurobiology of Disease

The Neural Signature of Impaired Inhibitory Control in Individuals with Heroin Use Disorder

Ahmet O. Ceceli,[1] Sarah G. King,[2] Natalie McClain,[1] Nelly Alia-Klein,[1,2] and Rita Z. Goldstein[1,2]
[1]Department of Psychiatry, Icahn School of Medicine at Mount Sinai, New York, New York 10029, and [2]Department of Neuroscience, Friedman Brain Institute, Icahn School of Medicine at Mount Sinai, New York, New York 10029

Heroin addiction imposes a devastating toll on society, with little known about its neurobiology. Excessive salience attribution to drug over nondrug cues/reinforcers, with concomitant inhibitory control decreases, are common mechanisms underlying drug addiction. Although inhibitory control alterations generally culminate in prefrontal cortex (PFC) hypoactivations across drugs of abuse, patterns in individuals with heroin addiction (iHUDs) remain unknown. We used a stop-signal fMRI task designed to meet recent consensus guidelines in mapping inhibitory control in 41 iHUDs and 24 age- and sex-matched healthy controls (HCs). Despite group similarities in the stop-signal response time (SSRT; the classic inhibitory control measure), compared with HCs, iHUDs exhibited impaired target detection sensitivity (proportion of hits in go vs false alarms in stop trials; $p = 0.003$). Additionally, iHUDs exhibited lower right anterior PFC (aPFC) and dorsolateral PFC (dlPFC) activity during successful versus failed stops (the hallmark inhibitory control contrast). Lower left dlPFC/supplementary motor area (SMA) activity was associated with slower SSRT specifically in iHUDs and lower left aPFC activity with worse target sensitivity across all participants ($p < 0.05$ corrected). Importantly, in iHUDs, lower left SMA and aPFC activity during inhibitory control was associated with shorter time since last use and higher severity of dependence, respectively ($p < 0.05$ corrected). Together, results revealed lower perceptual sensitivity and hypoactivations during inhibitory control in cognitive control regions (e.g., aPFC, dlPFC, SMA) as associated with task performance and heroin use severity measures in iHUDs. Such neurobehavioral inhibitory control deficits may contribute to self-control lapses in heroin addiction, constituting targets for prevention and intervention efforts to enhance recovery.

Key words: **cognitive control; opiate; prefrontal cortex; response inhibition; stop-signal task; substance use disorder**

Significance Statement

Heroin addiction continues its deadly impact, with little known about the neurobiology of this disorder. Although behavioral and prefrontal cortical impairments in inhibitory control characterize addiction across drugs of abuse, these patterns remain underexplored in heroin addiction. Here, we illustrate a significant behavioral impairment in target discrimination in individuals with heroin addiction compared with matched healthy controls. We further show lower engagement during inhibitory control in the anterior and dorsolateral prefrontal cortex (key regions that regulate cognitive control) as associated with slower stopping, worse discrimination, and heroin use measures. Mapping the neurobiology of inhibitory control in heroin addiction for the first time, we identify potential treatment targets inclusive of prefrontal cortex-mediated cognitive control amenable for neuromodulation en route to recovery.

Introduction

More than 100,000 people have lost their lives to a drug overdose in 2021, mostly driven (>75%) by opioids (e.g., heroin; https://www.cdc.gov/nchs/pressroom/nchs_press_releases/2021/20211117.htm). Despite the devastating toll of heroin addiction on public health, the underlying neurobiology of this brain disease remains elusive. According to the impaired response inhibition and salience attribution model, individuals with drug addiction assign excessive salience to drug cues at the expense of nondrug reinforcers with concomitant decreases in inhibitory control (Goldstein and Volkow, 2002, 2011). As previously reviewed, neuroimaging studies that have targeted these

Received June 16, 2022; revised Sep. 26, 2022; accepted Sep. 28, 2022.

Author contributions: A.O.C., N.A., and R.Z.G. designed research; A.O.C., S.G.K., N.M., N.A., and R.Z.G. performed research; A.O.C., S.G.K., N.M., N.A., and R.Z.G. contributed unpublished reagents/analytic tools; A.O.C., S.G.K., and R.Z.G. analyzed data; A.O.C. and R.Z.G. wrote the paper.

This work was supported by National Institutes of Health–National Center for Complementary and Integrative Health Grant 1R01AT010627 to R.Z.G. We thank Greg Kronberg, Yuefeng Huang, Pierre-Olivier Gaudreault, Pias Malaker, Amelia Brackett, Gabriela Hoberman, Devarshi Vasa, Defne Ekin, and Alan Charles for assistance in data collection.

The authors declare no competing financial interests.

Correspondence should be addressed to Rita Z. Goldstein at rita.goldstein@mssm.edu.

https://doi.org/10.1523/JNEUROSCI.1237-22.2022

core symptoms of drug addiction indeed indicate lower prefrontal cortex (PFC) functioning during inhibitory control (Luijten et al., 2014; Zilverstand et al., 2018; Ceceli et al., 2022a), especially in the cognitive control network of the brain inclusive of the dorsolateral PFC (dlPFC), inferior frontal gyrus (IFG), supplementary motor area (SMA), and anterior cingulate cortex (ACC; Cole and Schneider, 2007).

Specifically, functional MRI (fMRI) studies in individuals with drug addiction mostly used Go/No-Go tasks that approximate components of inhibitory control processes, reporting hypoactivations in dlPFC, IFG, and ACC in nicotine (Nestor et al., 2011; Luijten et al., 2013); dlPFC, ACC, and anterior PFC (aPFC) in cannabis (Eldreth et al., 2004; Kober et al., 2014) and alcohol (Czapla et al., 2017); and dlPFC, IFG, SMA/pre-SMA, ACC, and aPFC in cocaine (Kaufman et al., 2003; Hester and Garavan, 2004) use disorders. The evidence for similarly altered inhibitory control-related neural function in individuals with heroin use disorder (iHUDs), or any other opioid, is limited. A study in 13 individuals with opioid use disorder (not heroin specific) reported Go/No-Go false-alarm-related ACC hypoactivity (Forman et al., 2004). Lower cognitive control network activity during a modified Go/No-Go task was associated with higher addiction severity in 26 individuals with opioid use disorder (Shi et al., 2021). In heroin use disorder, a single study used a Go/No-Go block design in 30 abstinent individuals in treatment and 18 healthy controls (HCs), reporting lower dlPFC, IFG, and ACC activity during Go/No-Go compared with only Go blocks and slower response times to the Go stimuli in the former group (Fu et al., 2008).

Although the Go/No-Go task is a well-validated and appropriate paradigm for capturing response selection (Raud et al., 2020), the No-Go signal onset does not induce a competition between response selection and suppression, rendering the task incomplete in estimating stopping ability following the initiation of a response—a core element of cognitive control (Aron, 2007) and the drug addiction phenomenology (Ersche et al., 2012; for review, see Goldstein and Volkow, 2002). The stop-signal task (SST) creates a competition between response initiation and inhibition (the horse-race model of go/stop processes; Logan and Cowan, 1984), allowing to effectively estimate the neurobehavioral signatures of inhibitory control (Verbruggen and Logan, 2008). The SST has informed the neural processes underlying stopping in substance use disorders, showing lower activation in the dorsomedial PFC/ACC in nicotine (de Ruiter et al., 2012), dlPFC and SMA in alcohol (Li et al., 2009; Sjoerds et al., 2014; Hu et al., 2015), and dlPFC, aPFC, SMA, and ACC (as well as in their networks) in cocaine (Li et al., 2008; Wang et al., 2018; Zhang et al., 2018; Ceceli et al., 2022b) addictions. However, these PFC impairments and their behavioral and drug-use-related correlates have yet to be extended to iHUDs. Here, we used an SST designed accordingly to previously published consensus parameters (Verbruggen et al., 2019) administered during fMRI to inpatient iHUDs compared with matched HCs. We focused on three core hypotheses; that is, compared with HCs, (1) iHUDs would exhibit impaired behavioral performance (stopping latency or another relevant task measure, signal detection sensitivity); (2) iHUDs would exhibit hypoactivations in inhibitory control PFC signaling, which would also be associated with worse behavioral performance; and within iHUDs, (3) inhibitory control behavior and/or PFC activity abnormalities would be associated with higher heroin use severity measures.

Table 1. Sample profile

Variable	HCs ($n = 24$)	iHUDs ($n = 41$)	Significance test
Age	41.7 (11.3)	40.9 (9.20)	$t_{(40.64)} = 0.30$, $p = 0.764$
Sex			Fisher's exact $p = 0.368$
Female	9 (37.5%)	9 (22.0%)	
Male	15 (62.5%)	31 (75.6%)	
Other	0 (0.0%)	1 (2.4%)	
Race			χ^2 (2,59) = 6.84, $p = 0.033$
Black	7 (29.2%)	2 (4.9%)	
White	13 (54.2%)	29 (70.7%)	
Other	3 (12.5%)	5 (12.2%)	
Unreported	1 (4.17%)	5 (12.2%)	
Education	16.5 (3.1)	12.1 (2.1)	$t_{(36.51)} = 6.14$, $p < 0.001$*
Verbal IQ	111 (7.6)	94.3 (11.8)	$t_{(62.36)} = 6.78$, $p < 0.001$*
Nonverbal IQ	12.1 (3.3)	10.1 (3.4)	$t_{(49.46)} = 2.34$, $p = 0.024$
Handedness (right/left)	19/5	33/8	χ^2 (1,65) = 0.02, $p = 0.898$
Beck's Depression Inventory-II	3.0 (4.5)	13.4 (12.1)	$t_{(55.78)} = 4.98$, $p < 0.001$*
Smoking status (current/past/never)	1/3/20	40/1/0	Fisher's exact $p < 0.001$*
Regular marijuana use in years	0.88 (1.78)	7.50 (8.38)	$t_{(45.89)} = 4.87$, $p < 0.001$*
Alcohol use (to intoxication) in years	5.75 (11.3)	5.85 (8.14)	$t_{(37.01)} = 0.04$, $p = 0.969$
Lifetime heroin use in years	–	11.0 (7.32)	
Days since last heroin use	–	187 (229)	
Heroin Craving Questionnaire	–	42.0 (16.1)	
Subjective Opiate Withdrawal Scale	–	3.12 (3.35)	
Severity of Dependence Scale	–	10.9 (3.66)	
Heroin use (days) in past 30 d	–	0.29 (1.12)	

Significant group differences (corrected for familywise error, $\alpha = 0.05/10 = 0.005$; cigarette smoking excluded from correction given the almost parallel distribution matching group identity) are flagged with an asterisk. Values in parentheses denote SD. Dashes in Table 1 represent "not applicable" as the heroin use variables do not pertain to the HCs.

Materials and Methods

Participants

A total of 41 iHUDs (40.9, SD = 9.2 years, 9 women) were recruited from an inpatient drug addiction rehabilitation facility (Samaritan Daytop Village, Queens, New York) and 24 age- and sex-matched HCs (41.7, SD = 11.3 years, 9 women) were recruited through advertisements and word of mouth in the surrounding community for matching purposes. Table 1 provides a complete sample profile. The Icahn School of Medicine at Mount Sinai Institutional Review Board approved study procedures, and all participants provided written informed consent.

A comprehensive clinical diagnostic interview was conducted, consisting of the Mini International Neuropsychiatric Interview, seventh edition (Sheehan et al., 1998), and the Addiction Severity Index, fifth edition (McLellan et al., 1992), to assess the severity of lifetime and recent alcohol- and drug-related problems. Craving and withdrawal symptoms were determined using the Heroin Craving Questionnaire (a modified version of the Cocaine Craving Questionnaire; Tiffany et al., 1993) and the Subjective Opiate Withdrawal Scale (Handelsman et al., 1987), respectively. The severity of drug dependence was measured using the Severity of Dependence Scale (Gossop et al., 1992). Severity of nicotine dependence was measured using the Fagerström Test for Nicotine Dependence (Heatherton et al., 1991). All iHUDs met criteria for HUD (primary route of administration, 24 intravenous; 13 nasal; 3 smoked/inhaled; 1 oral). Other comorbidities in iHUDs included cocaine use disorder ($n = 9$), major depressive disorder ($n = 8$), post-traumatic stress disorder ($n = 5$), sedative use disorder ($n = 5$), alcohol use disorder ($n = 3$), polysubstance use disorder (i.e., dependence on at least three groups

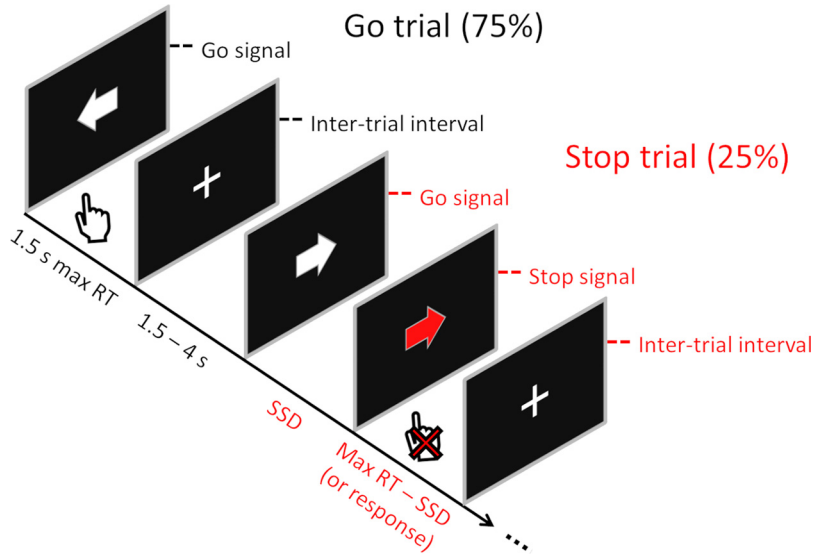

Figure 1. The stop-signal task. Participants are instructed to make directional responses as quickly and accurately as possible to the white arrow stimuli and suppress their responses when the arrow color turns to red after a variable delay (i.e., SSD). Figure adapted from Verbruggen et al. (2019) with permission. RT: response time; s: seconds.

of substances, not including nicotine and caffeine, in the past 12 months, with no single substance predominating; $n = 3$), generalized anxiety disorder ($n = 2$), marijuana use disorder ($n = 2$), meth/amphetamine use disorder ($n = 2$), panic disorder ($n = 2$), and obsessive-compulsive disorder ($n = 1$). All substance-use-related comorbidities commonly observed in individuals with drug addiction (27, 28) were either in partial or sustained remission at the time of the study. No current comorbidities were found in the HC group. All iHUDs were under medication-assisted treatment (as clinically determined), with urine toxicology positive for methadone ($n = 34$), buprenorphine ($n = 6$), or methadone and buprenorphine ($n = 1$).

Exclusion criteria for all participants were the following: (1) *Diagnostic and Statistical Manual of Mental Disorders*, fifth edition (DSM-5) diagnosis for schizophrenia or neurodevelopmental disorder (e.g., autism); (2) history of head trauma with loss of consciousness (>30 min); (3) history of neurologic disorders including seizures; (4) cardiovascular disease and/or other medical conditions, including metabolic, endocrinological, oncological, or autoimmune diseases, and infectious diseases such as Hepatitis B and C or HIV/AIDS; and (5) metal implants or other MR contraindications (including pregnancy). We did not exclude for DSM-5 diagnosis of a drug use disorder other than opiates as long as heroin was the primary drug of choice/reason for treatment seeking as iHUDs commonly use other drugs of abuse. Criteria for the HCs were the same, except current or a history of any drug use disorder was exclusionary. Forty of the 41 iHUDs and a single HC were current cigarette smokers (cigarettes smoked per day in iHUDs, 2.2, SD = 2.1; mean nicotine dependence score in iHUDs, 3.8, SD = 1.6). Neither group reported significant marijuana use in the past month (two recent users in HCs and one in iHUDs); however, the groups differed significantly in years of regular marijuana use (reported by seven HCs and 27 iHUDs; Table 1). The groups did not differ in years of alcohol use to intoxication (Table 1).

Experimental design and statistical analysis

The stop-signal task

Participants underwent a recently revised version of the SST STOP-IT (Verbruggen et al., 2008), which abides by the latest consensus guidelines in estimating inhibitory control (Verbruggen et al., 2019), that we modified for the fMRI context and presented via the JavaScript library jsPsych (de Leeuw, 2015; Fig. 1). In brief, participants were instructed to respond to the direction of the white arrows (left or right) that appeared on the screen over a black background using the corresponding buttons on the MR-compatible response glove (index or middle finger presses for right-handed, the reverse for left-handed; HCs, $n = 5$; iHUDs, $n = 8$ participants; no significant differences between groups in handedness, $p = 0.898$) as quickly and accurately as possible. Participants had a maximum response window of 1500 ms. These go trials comprised 75% of the task (144 trials). In the remaining 25% (48 trials), the white arrow (the go signal) changed to red (the stop signal) after a variable delay [the stop-signal delay (SSD)], to which participants were instructed to stop their response. The SSD was set to an initial duration of 200 ms and adjusted in parallel to the participant's stopping ability so that when the participant successfully stopped, the SSD increased by 50 ms (making the next stop trial more difficult), and when the participant failed to stop, the SSD decreased by 50 ms (making the next stop trial easier). Trials were separated by a jittered intertrial interval during which a fixation point was displayed (mean duration, 2750 ms; range, 1500–4000 ms) to minimize anticipatory effects and improve signal detection (Hagberg et al., 2001; Wager and Nichols, 2003). The task was administered over two fMRI scan runs, separated by a brief interval in which we displayed performance feedback in the form of average response time (RT) in ms, proportion of missed go trials, and proportion of correct stops. Participants were then reminded to avoid waiting for the stop signals and to respond quickly and accurately to the direction of the arrows before progressing to the next run to minimize task noncompliance (Verbruggen et al., 2019).

MRI data acquisition. MRI scans were acquired using a Siemens 3.0 Tesla Skyra with a 32-channel head coil. Anatomical T1-weighted images were obtained using the following parameters: 3D Magnetization-Prepared Rapid Gradient-Echo (MPRAGE) sequence with 256 × 256 × 179 mm^3 FOV, 0.8 mm isotropic resolution, TR/TE/TI = 2400/2.07/1000 ms, 8° flip angle with binomial (1, −1) fat saturation, 240 Hz/pixel bandwidth, 7.6 ms echo spacing, and in-plane acceleration [GRAPPA (generalized autocalibrating partially parallel acquisitions)] factor of 2, approximate acquisition time of 7 min. The blood-oxygen-level-dependent (BOLD) fMRI responses were measured as a function of time using T2*-weighted single-shot multiband accelerated (factor of 7) gradient-echo echoplanar image sequence [TE/TR = 35/1000 ms, 2.1 isotropic mm resolution, 70 axial slices without gaps for whole-brain coverage (147 mm), FOV 206 × 181 mm, matrix size 96 × 84, 60° flip angle (approximately Ernst angle), blipped CAIPIRINHA (Controlled Aliasing in Parallel Imaging Results in Higher Acceleration) phase-encoding shift = FOV/3, 1860 kHz/pixel bandwidth with ramp sampling, echo spacing 0.68 ms, and echo train length 84 ms]. Each of the two functional runs were ~6 min 30 s (total task duration ~13 min). The 1.5 h scan session included additional structural and functional procedures to be reported elsewhere.

MRI data preprocessing. Raw functional and structural MRI data in DICOM (Digital Imaging and Communications in Medicine) format were converted to NIFTI (Neuroimaging Informatics Technology Initiative) using the dcm2niix tool (Li et al., 2016). These data were preprocessed via the Nipype-based fMRIPrep pipeline (version 20.2.3; Gorgolewski et al., 2011; Esteban et al., 2019). FMRIPrep is an fMRI preprocessing pipeline that uses tools from well-established neuroimaging software [e.g., Functional MRI of the Brain (FMRIB) Software Library (FSL), FreeSurfer, and Advanced Normalization Tools (ANTs)] for optimal and standardized fMRI preprocessing; Esteban et al., 2019]. Structural images were intensity normalized and skull stripped using ANTs (Tustison et al., 2010). These images were spatially normalized to the International Consortium for Brain Mapping 152 nonlinear asymmetrical template using ANTs via nonlinear registration (Avants et al., 2008; Fonov et al., 2009). Brain tissue segmentation was conducted using FSL FAST (FMRIB Automated Segmentation Tool; Zhang et al., 2001) to derive white matter, gray matter, and cerebrospinal fluid estimates. Functional data were corrected for motion artifacts using FSL MCFLIRT (FMRIB Linear Image Registration Tool with motion correction) and

for distortion using spin-echo field maps acquired in opposing phase encoding directions via the AFNI (Analysis of Functional Neuro Images) 3dQwarp function (Cox, 1996; Jenkinson et al., 2002). Motion- and distortion-corrected images were coregistered to the participant's structural images using boundary-based registration with nine degrees of freedom via FSL FLIRT (Jenkinson and Smith, 2001; Fonov et al., 2009). These correction, transformation, and registration steps were integrated into a single-step transformation workflow using ANTs, resampled to isotropic voxels of 2 mm. The following confounds were extracted from fMRIPrep as time-series for each BOLD scan run: six translation and rotation parameters (x, y, and z for each) as motion regressors, global CSF and white matter components, and cosine regressors for high-pass filtering (128 s cutoff) to ignore low-frequency drift related to scanner and physiological noise. The preprocessed data from the fMRIPrep pipeline were spatially smoothed using a Gaussian kernel (5 mm full-width at half-maximum) to improve signal-to-noise ratio. Groups were significantly different in motion during the task (iHUDs greater than HCs; mean framewise displacement in iHUDs = 0.259 mm; in HCs = 0.197 mm, $t_{(57)} = 2.00$, $p = 0.020$). Framewise displacement did not correlate with inhibitory control brain activity in HCs ($p = 0.696$) or iHUDs ($p = 0.849$).

Behavioral data analysis. The estimation of inhibitory control via the stop-signal RT (SSRT) relies on the assumption that the go and stop processes compete for control over behavior (i.e., the horse-race model of response inhibition; Logan and Cowan, 1984). To ensure a valid estimate of inhibitory control, we followed well-established parameters for upholding the validity of the horse-race model in SST data analyses (Verbruggen et al., 2019). In compliance with these recommendations, we calculated SSRT using the package Analyze-it (Verbruggen et al., 2019). Using the integration method, Analyze-it identifies the nth RT in the Go RT distribution (n being the number of Go RTs multiplied by the proportion of incorrect stops). The nth RT represents the end of the stopping process, improving on practices that use mean RT to represent this marker (Verbruggen et al., 2019). SSRT is then calculated by subtracting mean SSD from the nth RT, with higher SSRT indicating slower stopping latency (worse performance). We further inspected SST performance via signal detection theory (Stanislaw and Todorov, 1999), supplementing the degree of inhibitory control quantified by SSRT with d', a measure of sensitivity in detecting targets (here, go trials) over nontargets (stop trials). We calculated d' by Z-transforming hit (proportion of correct responses to go trials) and false alarm (proportion of responses following a stop-signal) rates, with higher d' values reflecting higher sensitivity.

We compared behavioral performance in the stop-signal task (i.e., stop accuracy, go accuracy, SSRT, SSD, go RT, and d') between groups, corrected for familywise error ($\alpha = 0.05/6 = 0.008$) using Welch's two-sample t tests to minimize Type I error in unbalanced samples (Ruxton, 2006; Derrick and White, 2016). We calculated go accuracy rates as correct go responses divided by the total of correct and incorrect go responses (i.e., accounting for directional errors). We further explored via linear models potential associations between the SSRT and d' with heroin use severity measures of interest in Table 1 (i.e., lifetime heroin use, days since last use, heroin craving, withdrawal, and severity of dependence, corrected for familywise error, $\alpha = 0.05/5 = 0.01$). Because of lack of variability in frequency of recent heroin use (all iHUDs resided in an inpatient setting with most reporting no recent use in the past month), we did not inspect correlations with this variable. Within iHUDs, correlations were also inspected with nicotine dependence and cigarettes smoked per day to determine whether these variables of no interest significantly contributed to the results. To account for the contribution of other potentially explanatory variables, we first compared iHUDs and HCs in demographic, neuropsychological, and commonly used drug measures outlined in Table 1 (i.e., age, sex, race, education, verbal IQ, nonverbal IQ, handedness, depression symptoms, regular use of marijuana, and years of alcohol use to intoxication) using Welch's two-sample t tests, chi-square tests, or Fisher's exact tests, where appropriate, corrected for familywise error ($\alpha = 0.05/10 = 0.005$; cigarette smoking measures were excluded given the almost parallel distribution matching group identity). Those variables showing significant group differences were tested for their potential correlation with SSRT and d'. Variables that showed significant group differences and correlations with behavior were used as covariates in linear mixed models (SSRT or d' as dependent variable, group and the covariates as fixed factors, and participant as random factor) to correct for their potential contributions to the findings.

BOLD fMRI data analyses. Parameter estimates for each of the four task events (Go Success for successful go responses, Go Fail for missed go trials or directional errors, Stop Success for successful inhibitions following a stop signal, and Stop Fail for failed inhibition following a stop signal) and their temporal derivatives were modeled and entered into a general linear model (GLM) using FSL FEAT (fMRI Expert Analysis Tool; version 5.98; Woolrich et al., 2001). These regressors were sampled from the onset of the go signals of the corresponding trials (the white arrow) using 1.5 s events and convolved with a canonical hemodynamic response function. Intertrial intervals contributed to the task baseline (Aron and Poldrack, 2006). We used Go Fail events and fMRIPrep confound time series (details provided in the section *MRI data preprocessing*) as regressors of no interest.

In each run, we calculated the hallmark inhibitory control contrast, Stop Success > Stop Fail, in our first-level analyses to represent inhibitory control brain activity. Next, these run-level contrast estimates were entered into a fixed-effects model to average across runs to yield subject-level parameter estimates. To test group-level analyses of inhibitory control (HCs > iHUDs and iHUDs > HCs), we used FSL FLAME (FMRIB Local Analysis of Mixed Effects) 1 and 2, which improves variance estimations using Markov Chain Monte Carlo simulations and permits better population inferences (Beckmann et al., 2003). To minimize Type I error, we selected a priori a cluster defining threshold of $p < 0.001$, corrected to a cluster-extent threshold of $p < 0.05$, per recommended practices (Eklund et al., 2016).

To inspect the PFC activity related to behavioral inhibitory control performance, we separately performed similar higher-level analyses (i.e., same variance estimation and thresholding parameters) with the addition of SSRT and d' as covariates of interest. Given our a priori interest in the prefrontal correlates of inhibitory control, and after conducting the whole-brain analyses as described above for our main group level comparisons, we restricted the SSRT and d' correlation results to the PFC using small-volume correction and an anatomically defined PFC mask. This PFC mask of 37,876 voxels (20.8% of the whole-brain mask) encompassed the ventromedial PFC (vmPFC; inclusive of frontal medial and frontal orbital cortices), dorsomedial PFC/paracingulate, IFG (inclusive of pars opercularis and triangularis subregions), dlPFC/middle frontal gyrus, and aPFC/frontal pole, derived from the Harvard-Oxford Cortical Atlas with a 25% probabilistic threshold applied to each region. Comparing slopes to inspect regions that showed iHUD- or HC-specific correlations, we tested for group differences in these task-behavior/PFC correlations; we also inspected correlations across all participants for potential general relationships with behavioral estimates. Finally, we followed the steps outlined above (under correlations with task performance) for inspecting the potential influence on PFC activity during inhibitory control (using the same PFC mask) of the select demographic, neuropsychological, and commonly used drugs (listed above). Specifically, correlations among the variables that showed significant differences between the groups were inspected with peak BOLD activity during inhibitory control; those showing significant associations were entered into the GLMs as covariates. Nicotine dependence and the number of cigarettes smoked per day were similarly inspected in the iHUDs. We further inspected potential PFC associations with heroin use variables in separate higher-level GLM analyses to avoid multicollinearity (corrected for familywise error, $\alpha = 0.05/5 = 0.01$). Across all analyses, values that were 2 SDs above or below the mean were identified as outliers, and the affected tests are reported with and without their inclusion. Correlational analyses including these outliers were supplemented with robust regression coefficients for completeness. Behavioral- and heroin-use-related correlations were repeated using a whole-brain mask for exploratory inspections of potential associations outside our PFC focus.

Results

Participants

The groups were comparable in age, sex, race, and nonverbal IQ. Significant group differences were noted in years of education,

Table 2. Behavioral performance in the stop-signal task

Variable	HCs ($n = 24$)	iHUDs ($n = 41$)	Significance test	Effect size (Cohen's d)	95% CI
Stop accuracy	0.48 (0.04)	0.47 (0.07)	$t_{(62.99)} = 0.59$, $p = 0.556$	$d = 0.134$	−0.02, 0.03
Go accuracy	0.98 (0.02)	0.95 (0.05)	$t_{(60.92)} = 2.95$, $p = 0.004$*	$d = 0.640$	0.01, 0.04
SSRT	277 (40.9)	276 (67.0)	$t_{(62.85)} = 0.05$, $p = 0.960$	$d = 0.012$	−26.10, 27.40
SSD	288 (94.8)	313 (143)	$t_{(61.91)} = 0.83$, $p = 0.412$	$d = 0.191$	−83.50, 34.60
Go RT	585 (83.3)	633 (131)	$t_{(62.48)} = 1.79$, $p = 0.078$	$d = 0.411$	−100.71, 5.51
d'	0.62 (0.04)	0.57 (0.08)	$t_{(62.80)} = 3.07$, $p = 0.003$*	$d = 0.683$	0.02, 0.08

Significant group differences (corrected for familywise error, $\alpha = 0.05/6 = 0.008$) are flagged with an asterisk. Values in parentheses denote SD. Go accuracy was calculated as go responses divided by the total of correct and incorrect go responses.

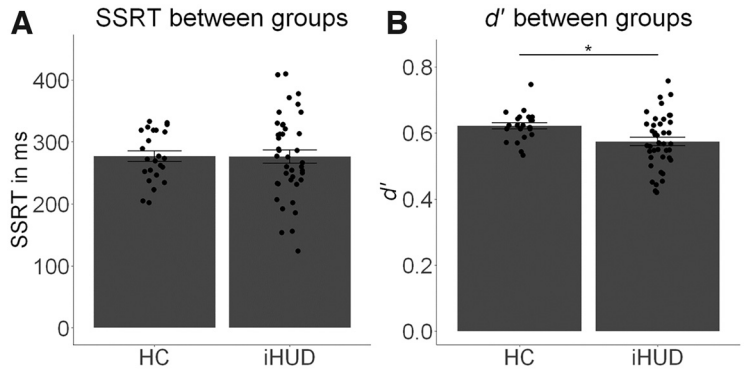

Figure 2. Stop-signal task performance. ***A***, ***B***, iHUD and HC participants' (***A***) SSRT (the classic inhibitory control measure of stopping latency), indicating no significant group differences ($p = 0.960$) and (***B***) target detection sensitivity (d'), indicating significantly lower d' in iHUDs compared with HCs ($p = 0.003$). Swarm plots indicate individual data points. Error bars indicate SEM. No data points were 3 SDs above or below the mean. Significant group difference flagged with an asterisk.

verbal IQ (HCs greater than iHUDs), depression symptoms (iHUDs greater than HCs), nicotine smoking status, and regular marijuana use (all p values < 0.001; $\alpha = 0.005$; Table 1).

Behavioral results

A Welch's two sample t test revealed significantly lower mean go accuracy in iHUDs compared with HCs, $t_{(60.92)} = 2.95$, $p = 0.004$ ($\alpha = 0.008$), Cohen's $d = 0.640$. Nevertheless, all subjects met the recommended performance thresholds (i.e., mean go accuracy greater than or equal 60%, mean stop accuracy greater than or equal 25 and less than or equal to 75%, and SSRT greater than 0). There were no significant differences between iHUDs and HCs in SSRT, $t_{(62.8)} = 0.05$, $p = 0.960$, Cohen's $d = 0.012$ (Fig. 2, left). However, iHUDs exhibited significantly lower sensitivity in detecting targets over nontargets, $t_{(62.8)} = 3.07$, $p = 0.003$ ($\alpha = 0.008$), Cohen's $d = 0.683$ (Fig. 2, right, Table 2 for all behavioral performance measures). Neither SSRT nor d' correlated with the heroin use severity measures (all p values > 0.184). Education, verbal IQ, depression symptoms, or years of regular marijuana use did not significantly correlate with SSRT (all p values in iHUDs > 0.440, all p values in HCs > 0.155) or d' (all p values in iHUDs > 0.296, all p values in HCs > 0.331). Similarly, neither SSRT (all p values > 0.138) nor d' ($p > 0.219$) significantly correlated with nicotine dependence scores or number of cigarettes smoked/day in iHUDs.

BOLD fMRI results

Inhibitory control brain activity. Whole-brain analyses that interrogated the inhibitory control contrast (Stop Success > Stop Fail) across all participants revealed significant activations in the classical inhibitory control-associated regions including the right SMA/dlPFC [Brodmann's area (BA) 6], bilateral lateral aPFC (BA 10), left vmPFC/orbitofrontal PFC (BA 11), among others (Fig. 3, Table 3).

Whole-brain analyses that interrogated group differences in inhibitory control brain activity revealed significantly lower Stop Success > Stop Fail signaling in iHUDs compared with HCs in the right lateral aPFC (BA 10; Montreal Neurological Institute [MNI] space 26, 60, 0; peak $Z = 4.49$, $p = 0.001$, 97 voxels; Fig. 4, middle) and the right dlPFC (BA 9; MNI space 36, 26, 32; peak $Z = 4.49$, $p = 0.015$, 65 voxels; Fig. 4, right). No region showed significantly higher activity in iHUDs compared with HCs.

Education, verbal IQ, depression symptoms, or years of regular marijuana use did not significantly correlate with inhibitory control brain activity (all p values in iHUDs > 0.531, all p values in HCs > 0.276). Similarly, nicotine dependence scores or number of cigarettes smoked/day in iHUDs did not correlate with inhibitory control brain activity (all p values > 0.751).

Brain and behavioral performance correlations. Using our a priori mask, we found that lower activations in the left dlPFC/SMA (BA 6; MNI space −38, 0, 64; peak $Z = 4.84$, $p = 0.020$, 41 voxels) and right IFG, pars opercularis (BA 44; MNI space 50, 14, 28; peak $Z = 4.13$, $p = 0.037$, 35 voxels), were associated with slower SSRT in iHUDs compared with HCs. This difference between slopes was driven by the association between lower left dlPFC/SMA activity (BA 6; MNI space −30, 6, 62; peak $Z = 4.62$, $p = 0.028$, 38 voxels) and slower SSRT in iHUDs (Fig. 5; no significant clusters driven by the HC group), suggesting that dlPFC/SMA engagement may be especially important in driving stopping latency in iHUDs. SSRT did not correlate with inhibitory control prefrontal activity across all participants.

Exploratory whole-brain correlations of SSRT revealed that lower activity in the right supramarginal gyrus (BA 7; MNI space 38, −44, 42; peak $Z = 5.19$, $p = 0.011$, 69 voxels) was associated with slower SSRT in iHUDs compared with HCs. When inspected within each group, no significant correlations survived in HCs, whereas the iHUDs showed a significant relationship between lower activity in the right lateral occipital cortex (BA 19; MNI space 38, −84, 24; peak $Z = 4.27$, $p = 0.001$, 101 voxels) and slower SSRT. Whole-brain correlations did not reveal significant associations with SSRT across all participants.

Using our mask, we also searched for PFC correlations with d' during inhibitory control. There were no significant group differences in associations between inhibitory control brain activity and d'. Across all participants, lower activity in the left lateral aPFC (BA 10; MNI space −20, 58, 16; peak $Z = 4.99$, $p = 0.013$, 46 voxels) correlated with lower d' (worse sensitivity; Fig. 6).

Exploratory whole-brain correlations of d' revealed that lower activity in the right lateral occipital cortex (BA 39; MNI space 34,

56, 40; peak $Z = 4.93$, $p < 0.001$, 116 voxels) and left supramarginal gyrus (BA 39; MNI space −32, −50, 40; peak $Z = 5.20$, $p = 0.006$, 77 voxels) were associated with lower d' in HCs compared with iHUDs. When inspected within each group, the HCs showed a significant relationship between lower activity in the right lateral aPFC/dlPFC (BA 9; MNI space 32, 36, 22; peak $Z = 4.36$, $p = 0.003$, 78 voxels) and in the right lateral occipital cortex (BA 39; MNI space 34, −56, 40; peak $Z = 4.26$, $p = 0.014$, 59 voxels) and lower d', whereas no significant correlations were found in iHUDs. Whole-brain correlations did not reveal significant associations with d' across all participants.

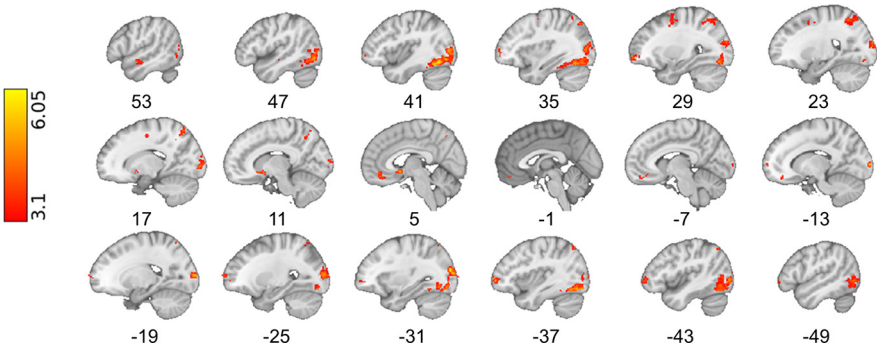

Figure 3. Inhibitory control brain activity recruited by the task. Across all participants, the stop-signal task elicited higher activity in the right supplementary motor area/dorsolateral prefrontal cortex, right lateral anterior prefrontal cortex, and left ventromedial/orbitofrontal prefrontal cortex, among others (Table 3) during successful versus failed stops (the hallmark inhibitory control contrast). Significant results were detected using a cluster-defining threshold of $Z > 3.1$, corrected to $p < 0.05$. The labels below each slice indicate *x*-axis coordinates in the MNI-152 space.

Heroin use severity and inhibitory control brain activity in iHUDs. Fewer days since last use was associated with lower left SMA activity (BA 6; MNI space −4, 12, 62; peak $Z = 3.82$, $p = 0.003$, 62 voxels) in iHUDs (Fig. 7*A*). The exclusion of two outliers in days since last use did not substantially affect these results ($R^2 = 0.34$, $p < 0.001$), and the exclusion of one outlier in SMA activity reduced this association to a trend level when accounting for five heroin use severity measures, $R^2 = 0.16$, $p = 0.012$, $\alpha = 0.01$. However, a robust regression conducted on this relationship that included the outliers revealed it remained significant when assuming a normal t distribution ($t = 4.908$, $\beta = 1.147$, SE = 0.23, $p < 0.001$). Higher severity of dependence scale scores were associated with lower activity in the left medial aPFC (BA 10; MNI space −16, 64, 10; peak $Z = 3.99$, $p < 0.001$, 133 voxels) and dorsal ACC (BA 32; MNI space 0, 52, 6; peak $Z = 4.23$, $p = 0.006$, 55 voxels).

Table 3. Inhibitory control brain activity (stop success > stop fail) across all participants

Region	Side	Voxels	Peak *Z*	*p*	*x*	*y*	*z*	BA
Anterior prefrontal cortex, lateral	L	59	4.22	0.025	−26	68	8	BA 10
Anterior prefrontal cortex, lateral	R	83	4.6	0.004	30	62	−6	BA 10
Anterior prefrontal cortex, lateral	L	179	4.97	<0.001	−34	56	0	BA 10
Ventromedial prefrontal cortex	L	127	4.57	<0.001	−4	50	−16	BA 11
Caudate	R	105	4.92	<0.001	6	10	−8	–
Superior temporal gyrus, anterior	R	90	4.29	0.002	60	−2	−10	BA 22
Supplementary motor area	R	179	5.13	<0.001	32	−4	48	BA 6
Lateral occipital cortex, superior	R	435	5.05	<0.001	28	−60	56	BA 7
Lateral occipital cortex, inferior	R	1534	6.05	<0.001	44	−64	−14	BA 19
Lateral occipital cortex, superior	L	77	4.46	0.006	−36	−70	52	BA 7
Lateral occipital cortex, inferior	L	1396	5.96	<0.001	−32	−88	18	BA 19

Coordinates are in the MNI-152 space. Data are resampled to isotropic voxel size of 2 mm. R, right; L, left. Dash represents "not applicable" as BA labels do not extend to the caudate.

Supporting our main findings using our a priori mask, the parallel exploratory whole-brain analyses revealed that fewer days since last use was associated with lower left SMA activity at a trend level when corrected for familywise error ($\alpha = 0.01$; BA 6; MNI space −8, 10, 60; peak $Z = 4.27$, $p = 0.011$, 69 voxels) in iHUDs. Also consistent with the main findings, higher severity of dependence scale scores were associated with lower activity in the left medial aPFC (BA 10; MNI space −16, 64, 10; peak $Z = 3.99$, $p < 0.001$, 151 voxels) and dorsal ACC (BA 32; MNI space 0, 52, 6; peak $Z = 4.23$, $p = 0.006$, 55 voxels). No brain regions significantly correlated with heroin withdrawal, lifetime heroin use, or craving.

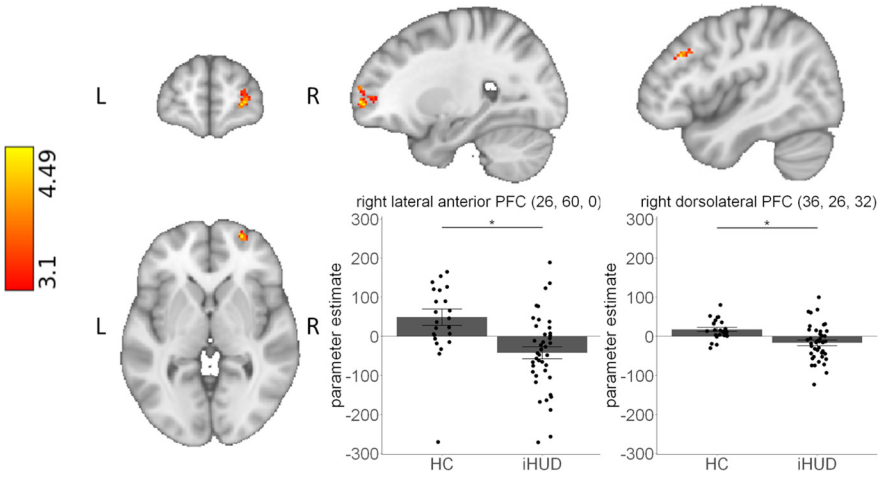

Figure 4. Group differences in inhibitory control brain activity. iHUDs, compared with HCs, exhibited significantly lower right lateral anterior PFC (left plot) and right dorsolateral PFC (right plot) activity during successful versus failed stops (the hallmark inhibitory control contrast). Significant results were detected using a cluster-defining threshold of $Z > 3.1$, corrected to $p < 0.05$. Bar plots indicate parameter estimates from the voxel with the peak *Z* score in each cluster. The right dorsolateral PFC cluster is depicted using its center of gravity for visualization purposes. Swarm plots indicate individual data points. Error bars denote SEM. No data points were 3 SDs above or below the mean. Coordinates are in the MNI-152 space. Significant group differences are flagged with an asterisk.

Discussion

Although lower inhibitory control PFC signaling in drug addiction is consistently reported across drug classes (for review, see Luijten et al., 2014; Zilverstand et al., 2018; Ceceli et al., 2022a), these patterns were yet to be extended to heroin (or any opioid) addiction. Here, using a well-accepted and optimized SST (Verbruggen et al., 2019), we mapped the neurobiological substrates of inhibitory control deficits in iHUDs. The task elicited cognitive control network activity across all participants as expected, with comparable SSRT between groups. Importantly, in support of our hypotheses,

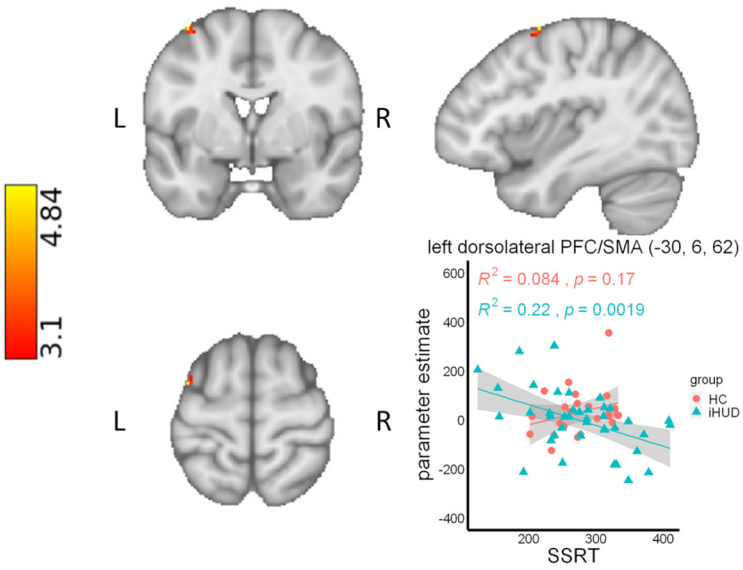

Figure 5. Prefrontal cortex correlations with stop-signal response time in iHUDs and HCs. A significant relationship between slower SSRT (the classic inhibitory control measure of stopping latency) and lower left dlPFC/supplementary motor area activity during successful compared with failed stops (the hallmark inhibitory control contrast) was evident specifically in iHUDs compared with HCs. Significant results were detected within a small volume corrected PFC mask, using a cluster-defining threshold of $Z > 3.1$, corrected to $p < 0.05$. No data points were 3 SDs above or below the mean. Coordinates are in the MNI-152 space.

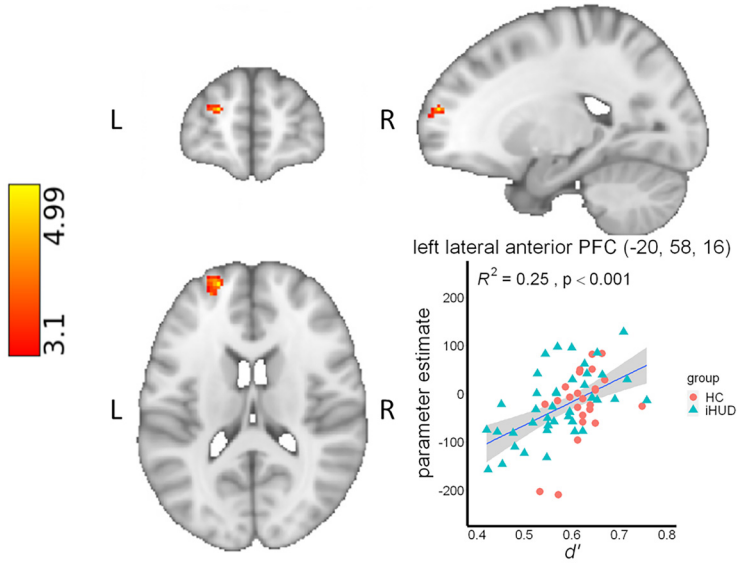

Figure 6. Prefrontal cortex correlations with target detection sensitivity in iHUDs and HCs. A significant relationship between worse target detection sensitivity (d') and lower left lateral aPFC activity during successful compared with failed stops (the hallmark inhibitory control contrast) was evident across all participants. Significant results were detected within a small volume corrected PFC mask, using a cluster-defining threshold of $Z > 3.1$, corrected to $p < 0.05$. No data points were 3 SDs above or below the mean. Coordinates are in the MNI-152 space.

(1) sensitivity to targets over nontargets was significantly lower in iHUDs compared with HCs, revealing an inhibitory performance impairment in the former; (2) right lateral aPFC and dlPFC activity was significantly lower in iHUDs compared with HCs. Lower left lateral aPFC and dlPFC/SMA signaling was associated with less sensitivity (across all subjects) and slower SSRT (specifically in iHUDs), respectively, suggesting that recruitment of these regions is key for behavioral performance, with the left dlPFC/SMA specifically regulating stopping speed in the iHUDs; and (3) in the iHUDs, fewer days since last use was associated with lower left SMA inhibitory control activity, and higher severity of dependence was associated with lower left medial aPFC activity, together suggesting that these abnormalities in inhibitory control PFC signaling are related to heroin use severity.

Although iHUDs may be generally expected to exhibit slower stopping latency than HCs, evidence in individuals with opioid use disorder that is based mostly on Go/No-Go tasks is both for (Fu et al., 2008; Rezvanfard et al., 2017) and against (Verdejo-García et al., 2007; Yang et al., 2009; Ahn and Vassileva, 2016) this expectation. In our study, the intact stop latency but impaired sensitivity in iHUDs alludes to a speed-accuracy trade-off, such that the iHUDs performed comparably to the HCs in stopping latency at the expense of target detection accuracy, as also evident in their impaired go accuracy. This finding is supported by comparable response latency but lower sensitivity in 13 methadone-maintained individuals with opioid addiction compared with 13 HCs as estimated using a Go/No-Go task (Forman et al., 2004). It is possible that medication-assisted treatment masks inhibitory slowing; although individuals with opioid dependence in protracted abstinence show prolonged SSRT compared with HCs, this deficit is not observed in those taking methadone (Liao et al., 2014). A closer inspection of the effects of medication-assisted treatment on SSRT will require larger samples including non-treatment-seeking iHUDs as well as those abstaining with and without medication assistance.

Importantly, for the first time we reveal lower PFC (specifically right lateral aPFC and dlPFC) engagement during inhibitory control in iHUDs, complementing the inhibitory control-related PFC hypoactivations commonly reported in other drug addictions (Li et al., 2008; de Ruiter et al., 2012; Sjoerds et al., 2014; Hu et al., 2015; Wang et al., 2018; Ceceli et al., 2022b). The aPFC in particular has been implicated in maintaining task rules and cognitive control over complex tasks (Braver et al., 2003; Sakai and Passingham, 2006; Cai and Leung, 2011). Individuals with cannabis or alcohol addiction exhibit lower aPFC signaling compared with HCs during the Stroop Color and Word Test (Kober et al., 2014; Hu et al., 2015), whereby one must override the prepotent reading response for color naming (Jensen and Rohwer, 1966). Although it is not a task that captures the stopping of an already initiated response, the Stroop task may overlap with the SST in maintaining task goals related to overriding prepotent responding. A related explanation for lower aPFC activity in our study invokes the role of this region in managing goals and subgoals (Koechlin et al., 1999). The SST demands participants to make quick

directional decisions in each trial (primary goal) with occasional suppressions of this response contingent on a stop signal (subgoal). Combined with the impaired target detection sensitivity in iHUDs, further showing a significant positive correlation with the aPFC in both groups, the inhibitory control-related aPFC hypoactivation may be a marker of a compromised ability to maintain multiple goals during a cognitively demanding, multitarget task. These deficits may be exacerbated with heroin use severity as reflected by the correlation between higher severity of dependence and lower aPFC function, further supported by our whole-brain explorations. The whole-brain correlations also indicated an association between lower activity in the right supramarginal gyrus and lateral occipital cortex and slower SSRT specifically in iHUDs, and lower target detection sensitivity specifically in the HCs. These regions are implicated in attentional processes (Murray and Wojciulik, 2004; Vossel et al., 2014) and show similar correlations with SSRT in the general population (Congdon et al., 2010; Ghahremani et al., 2012). The iHUDs may be engaging these attentional networks to maintain comparable stopping latency to that of the HCs, with no such compensatory mechanism in aiding target detection sensitivity, potentially contributing to the d' impairment in this group. However, these exploratory results beyond our PFC focus should be interpreted with caution and replicated in future investigations.

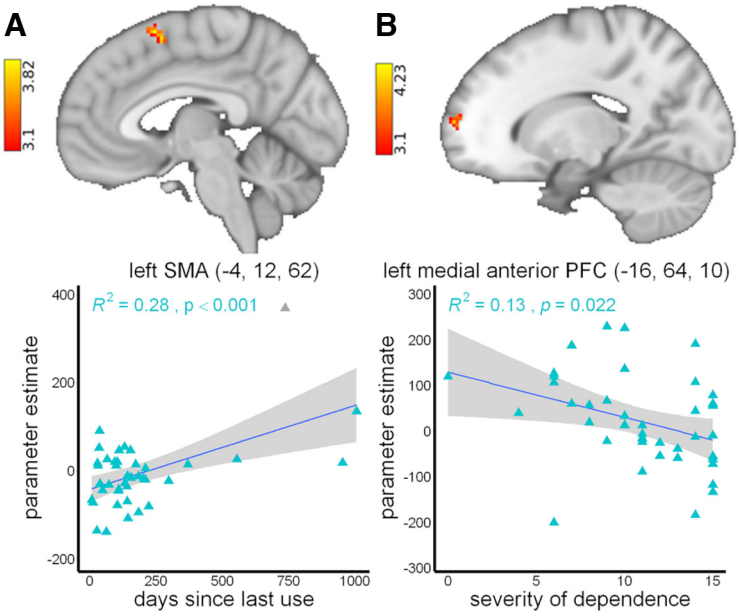

Figure 7. Prefrontal cortex correlations with heroin use severity measures in iHUDs. ***A***, ***B***, Fewer days since last use was associated with lower SMA activity (***A***), and higher severity of dependence was associated with lower aPFC activity (***B***) during successful compared with failed stops (the hallmark inhibitory control contrast) in iHUDs. Significant results were detected within a small volume corrected PFC mask, using a cluster-defining threshold of $Z > 3.1$, corrected for familywise error for five heroin use severity measures ($p < 0.05/5 = 0.01$). In ***A*** two participants' days since last use were 3 SDs above the mean. Excluding these outlier data points did not substantially affect the results ($R^2 = 0.34$, $p < 0.001$). One participant's SMA activity was identified as an outlier, and excluding this data point reduced this correlation to a trend level when accounting for five heroin use severity measures ($R^2 = 0.16$, $p = 0.012$, $\alpha = 0.01$). Nevertheless, a robust regression including the outliers supported the significant effect when assuming a normal t distribution ($t = 4.908$, $\beta = 1.147$, SE = 0.23, $p < 0.001$). The SMA outlier data point is denoted in gray, with the regression line reflecting all data points. Coordinates are in the MNI-152 space.

The lower inhibitory control activity in the dlPFC in iHUDs further suggests an altered neural signature of cognitive control in this group. As part of the dorsal attentional network, the dlPFC is thought to exert top-down modulation of selective attention to task-relevant perceptual input, as demonstrated in regulating control over conflicting visual stimuli (Egner and Hirsch, 2005; Gbadeyan et al., 2016). Inhibitory control-related dlPFC function is generally impaired in drug addiction (for review, see Zilverstand et al., 2018; Ceceli et al., 2022a), as characterized by hypoactivations during the SST and Stroop task in individuals with alcohol (Hu et al., 2015), cannabis (Kober et al., 2014), and cocaine use disorders (Moeller et al., 2014; Ceceli et al., 2022b). The lower dlPFC function in the iHUDs may underlie a maladaptive allocation of attentional resources to task-relevant information, which in real-world contexts may drive lapses in self-control, especially when drug cues bias attentional resources away from non-drug-related stimuli. The association between slower SSRT and lower dlPFC/SMA function in iHUDs is consistent with prior similar results in cocaine use disorder (Li et al., 2008). These results suggest a compensatory effect, where iHUDs may require higher dlPFC/SMA engagement to match HCs in stopping latency (but at the expense of accuracy). Reduced activations in the SMA, a region central to regulating inhibitory control (Aron and Poldrack, 2006; Cole and Schneider, 2007) and specifically driving motor planning (Tanji and Shima, 1994), as a function of fewer days since last heroin use suggest that the cognitive control network deficits in iHUDs may be labile and normalize with abstinence, as remains to be tested in larger and longitudinal efforts. Of note, inhibitory control group differences showed right-lateralized effects, consistent with the predominant recruitment of the right hemisphere by inhibitory control (for review, see Aron et al., 2014; but see also a lesion study suggesting the opposite, Swick et al., 2008). In contrast, the correlations with performance and heroin use severity measures were mostly localized to the left hemisphere (with bilateral subthreshold effects for correlations between higher severity of dependence/fewer days since last use and inhibitory control PFC activity). Goal maintenance during inhibitory control tasks may involve covert speech (e.g., inner reiteration of task goals; Tullett and Inzlicht, 2010; for review, see Alderson-Day and Fernyhough, 2015), which may have contributed to the left-lateralized inhibitory performance correlations and remains to be formally tested in drug addiction.

Several limitations should be considered when interpreting these findings. The groups showed significant differences in years of education, verbal IQ, depression scores, cigarette smoking, and years of regular marijuana use. Although these variables did not correlate with our dependent variables and thus could not have substantially contributed to the results, larger, more closely matched (e.g., in demographics, smoking status) samples may better tease apart the potential contributions of these individual differences. Although significant, the target detection sensitivity impairment in iHUDs was subtle as indicated by the medium effect size and should be replicated in future efforts. The need for larger sample sizes is especially pertinent for our correlational results. Although we generally found consistency between PFC-targeted and whole-brain correlations with the heroin use severity measures, the detection of whole-brain correlations with

behavioral performance measures may require higher powered studies, as brain and behavior associations have been show to require very large samples (Marek et al., 2022). As the PFC regions highlighted in these results encompass large, functionally heterogonous brain structures (Orr et al., 2015), further investigations are also needed to tease apart their additional functional roles. Future studies should also include more women to examine potential sex differences in inhibitory control function in iHUDs. Finally, the iHUDs were exclusively recruited from treatment facilities; future efforts should extend these results to both non-treatment-seeking and abstinent iHUDs to improve the generalization of findings.

To the best of our knowledge, this study marks the first investigation in iHUDs of inhibitory control performance and brain function, a core substrate underlying the human drug addiction experience. Our results indicate that consistent with impaired inhibitory control functions in substance use disorders across drug classes, iHUDs exhibit impaired inhibitory processes, that is, intact SSRT but impaired (yet subtle) sensitivity to detect targets over nontargets in an SST as associated with lower aPFC function when stopping, which in turn correlated with higher severity of dependence. Hypoactivations in the dlPFC (and SMA) correlated with slower (yet intact) stopping latency and with shorter time since last drug use. Overall, these results point to the neurobiological mechanisms that may underlie self-control lapses in individuals with heroin addiction. Importantly, these results identify potential treatment targets for improving inhibitory control functions in iHUDs, such as PFC-mediated cognitive strategies and/or neuromodulation to restore PFC cognitive control function en route to recovery.

References

Ahn W-Y, Vassileva J (2016) Machine-learning identifies substance-specific behavioral markers for opiate and stimulant dependence. Drug Alcohol Depend 161:247–257.

Alderson-Day B, Fernyhough C (2015) Inner speech: development, cognitive functions, phenomenology, and neurobiology. Psychol Bull 141:931–965.

Aron AR (2007) The neural basis of inhibition in cognitive control. Neuroscientist 13:214–228.

Aron AR, Poldrack RA (2006) Cortical and subcortical contributions to stop signal response inhibition: role of the subthalamic nucleus. J Neurosci 26:2424–2433.

Aron AR, Robbins TW, Poldrack RA (2014) Inhibition and the right inferior frontal cortex: one decade on. Trends Cogn Sci 18:177–185.

Avants BB, Epstein CL, Grossman M, Gee JC (2008) Symmetric diffeomorphic image registration with cross-correlation: evaluating automated labeling of elderly and neurodegenerative brain. Med Image Anal 12:26–41.

Beckmann CF, Jenkinson M, Smith SM (2003) General multilevel linear modeling for group analysis in FMRI. Neuroimage 20:1052–1063.

Braver TS, Reynolds JR, Donaldson DI (2003) Neural mechanisms of transient and sustained cognitive control during task switching. Neuron 39:713–726.

Cai W, Leung H-C (2011) Rule-guided executive control of response inhibition: functional topography of the inferior frontal cortex. PLoS One 6: e20840.

Ceceli AO, Bradberry CW, Goldstein RZ (2022a) The neurobiology of drug addiction: cross-species insights into the dysfunction and recovery of the prefrontal cortex. Neuropsychopharmacology 47:276–291.

Ceceli AO, Parvaz MA, King S, Schafer M, Malaker P, Sharma A, Alia-Klein N, Goldstein RZ (2022b) Altered prefrontal signaling during inhibitory control in a salient drug context in cocaine use disorder. Cereb Cortex 4: bhac087.

Cole MW, Schneider W (2007) The cognitive control network: integrated cortical regions with dissociable functions. Neuroimage 37:343–360.

Congdon E, Mumford JA, Cohen JR, Galvan A, Aron AR, Xue G, Miller E, Poldrack RA (2010) Engagement of large-scale networks is related to individual differences in inhibitory control. Neuroimage 53:653–663.

Cox RW (1996) AFNI: software for analysis and visualization of functional magnetic resonance neuroimages. Comput Biomed Res 29:162–173.

Czapla M, Baeuchl C, Simon JJ, Richter B, Kluge M, Friederich H-C, Mann K, Herpertz SC, Loeber S (2017) Do alcohol-dependent patients show different neural activation during response inhibition than healthy controls in an alcohol-related fMRI go/no-go-task? Psychopharmacology (Berl) 234:1001–1015.

de Leeuw JR (2015) jsPsych: a JavaScript library for creating behavioral experiments in a Web browser. Behav Res Methods 47:1–12.

Derrick B, White P (2016) Why Welch's test is Type I error robust. Quant Method Psycol 12:30–38.

de Ruiter MB, Oosterlaan J, Veltman DJ, van den Brink W, Goudriaan AE (2012) Similar hyporesponsiveness of the dorsomedial prefrontal cortex in problem gamblers and heavy smokers during an inhibitory control task. Drug Alcohol Depend 121:81–89.

Egner T, Hirsch J (2005) Cognitive control mechanisms resolve conflict through cortical amplification of task-relevant information. Nat Neurosci 8:1784–1790.

Eklund A, Nichols TE, Knutsson H (2016) Cluster failure: Why fMRI inferences for spatial extent have inflated false-positive rates. Proc Natl Acad Sci USA 113:7900–7905.

Eldreth DA, Matochik JA, Cadet JL, Bolla KI (2004) Abnormal brain activity in prefrontal brain regions in abstinent marijuana users. Neuroimage 23:914–920.

Ersche KD, Turton AJ, Chamberlain SR, Müller U, Bullmore ET, Robbins TW (2012) Cognitive dysfunction and anxious-impulsive personality traits are endophenotypes for drug dependence. Am J Psychiatry 169:926–936.

Esteban O, Markiewicz CJ, Blair RW, Moodie CA, Isik AI, Erramuzpe A, Kent JD, Goncalves M, DuPre E, Snyder M, Oya H, Ghosh SS, Wright J, Durnez J, Poldrack RA, Gorgolewski KJ (2019) fMRIPrep: a robust preprocessing pipeline for functional MRI. Nat Methods 16:111–116.

Fonov V, Evans A, McKinstry R, Almli C, Collins D (2009) Unbiased nonlinear average age-appropriate brain templates from birth to adulthood. Neuroimage 47:S102.

Forman SD, Dougherty GG, Casey BJ, Siegle GJ, Braver TS, Barch DM, Stenger VA, Wick-Hull C, Pisarov LA, Lorensen E (2004) Opiate addicts lack error-dependent activation of rostral anterior cingulate. Biol Psychiatry 55:531–537.

Fu LP, Bi GH, Zou ZT, Wang Y, Ye EM, Ma L, Fan M, Yang Z (2008) Impaired response inhibition function in abstinent heroin dependents: an fMRI study. Neurosci Lett 438:322–326.

Gbadeyan O, McMahon K, Steinhauser M, Meinzer M (2016) Stimulation of dorsolateral prefrontal cortex enhances adaptive cognitive control: a high-definition transcranial direct current stimulation study. J Neurosci 36:12530–12536.

Ghahremani DG, Lee B, Robertson CL, Tabibnia G, Morgan AT, Shetler ND, Brown AK, Monterosso JR, Aron AR, Mandelkern MA, Poldrack RA, London ED (2012) Striatal dopamine d2/d3 receptors mediate response inhibition and related activity in frontostriatal neural circuitry in humans. J Neurosci 32:7316–7324.

Goldstein RZ, Volkow ND (2002) Drug addiction and its underlying neurobiological basis: neuroimaging evidence for the involvement of the frontal cortex. Am J Psychiatry 159:1642–1652.

Goldstein RZ, Volkow ND (2011) Dysfunction of the prefrontal cortex in addiction: neuroimaging findings and clinical implications. Nat Rev Neurosci 12:652–669.

Gorgolewski K, Burns CD, Madison C, Clark D, Halchenko YO, Waskom ML, Ghosh SS (2011) Nipype: a flexible, lightweight and extensible neuroimaging data processing framework in Python. Front Neuroinform 5:13.

Gossop M, Griffiths P, Powis B, Strang J (1992) Severity of dependence and route of administration of heroin, cocaine and amphetamines. Br J Addict 87:1527–1536.

Hagberg GE, Zito G, Patria F, Sanes JN (2001) Improved detection of event-related functional MRI signals using probability functions. Neuroimage 14:1193–1205.

Handelsman L, Cochrane KJ, Aronson MJ, Ness R, Rubinstein KJ, Kanof PD (1987) Two new rating scales for opiate withdrawal. Am J Drug Alcohol Abuse 13:293–308.

Heatherton TF, Kozlowski LT, Frecker RC, Fagerström KO (1991) The Fagerström Test for Nicotine Dependence: a revision of the Fagerström Tolerance Questionnaire. Br J Addict 86:1119–1127.

Hester R, Garavan H (2004) Executive dysfunction in cocaine addiction: evidence for discordant frontal, cingulate, and cerebellar activity. J Neurosci 24:11017–11022.

Hu S, Ide JS, Zhang S, Sinha R, Li CR (2015) Conflict anticipation in alcohol dependence—a model-based fMRI study of stop signal task. Neuroimage Clin 8:39–50.

Jenkinson M, Smith S (2001) A global optimisation method for robust affine registration of brain images. Med Image Anal 5:143–156.

Jenkinson M, Bannister P, Brady M, Smith S (2002) Improved optimization for the robust and accurate linear registration and motion correction of brain images. Neuroimage 17:825–841.

Jensen AR, Rohwer WD (1966) The Stroop Color-Word Test: a review. Acta Psychol (Amst) 25:36–93.

Kaufman JN, Ross TJ, Stein EA, Garavan H (2003) Cingulate hypoactivity in cocaine users during a GO-NOGO task as revealed by event-related functional magnetic resonance imaging. J Neurosci 23:7839–7843.

Kober H, DeVito EE, DeLeone CM, Carroll KM, Potenza MN (2014) Cannabis abstinence during treatment and one-year follow-up: relationship to neural activity in men. Neuropsychopharmacology 39:2288–2298.

Koechlin E, Basso G, Pietrini P, Panzer S, Grafman J (1999) The role of the anterior prefrontal cortex in human cognition. Nature 399:148–151.

Li CR, Huang C, Yan P, Bhagwagar Z, Milivojevic V, Sinha R (2008) Neural correlates of impulse control during stop signal inhibition in cocaine-dependent men. Neuropsychopharmacology 33:1798–1806.

Li C-SR, Luo X, Yan P, Bergquist K, Sinha R (2009) Altered impulse control in alcohol dependence: neural measures of stop signal performance. Alcohol Clin Exp Res 33:740–750.

Li X, Morgan PS, Ashburner J, Smith J, Rorden C (2016) The first step for neuroimaging data analysis: DICOM to NIfTI conversion. J Neurosci Methods 264:47–56.

Liao D-L, Huang C-Y, Hu S, Fang S-C, Wu C-S, Chen W-T, Lee TS-H, Chen P-C, Li C-SR (2014) Cognitive control in opioid dependence and methadone maintenance treatment. PLoS One 9:e94589.

Logan G, Cowan W (1984) On the ability to inhibit thought and action: a theory of an act of control. Psychol Rev 91:295–327.

Luijten M, Veltman DJ, Hester R, Smits M, Nijs IMT, Pepplinkhuizen L, Franken IHA (2013) The role of dopamine in inhibitory control in smokers and non-smokers: a pharmacological fMRI study. Eur Neuropsychopharmacol 23:1247–1256.

Luijten M, Machielsen MWJ, Veltman DJ, Hester R, de Haan L, Franken IHA (2014) Systematic review of ERP and fMRI studies investigating inhibitory control and error processing in people with substance dependence and behavioural addictions. J Psychiatry Neurosci 39:149–169.

Marek S, et al. (2022) Reproducible brain-wide association studies require thousands of individuals. Nature 603:654–660.

McLellan AT, Kushner H, Metzger D, Peters R, Smith I, Grissom G, Pettinati H, Argeriou M (1992) The fifth edition of the Addiction Severity Index. J Subst Abuse Treat 9:199–213.

Moeller SJ, Konova AB, Parvaz MA, Tomasi D, Lane RD, Fort C, Goldstein RZ (2014) Functional, structural, and emotional correlates of impaired insight in cocaine addiction. JAMA Psychiatry 71:61–70.

Murray SO, Wojciulik E (2004) Attention increases neural selectivity in the human lateral occipital complex. Nat Neurosci 7:70–74.

Nestor L, McCabe E, Jones J, Clancy L, Garavan H (2011) Differences in "bottom-up" and "top-down" neural activity in current and former cigarette smokers: evidence for neural substrates which may promote nicotine abstinence through increased cognitive control. Neuroimage 56:2258–2275.

Orr JM, Smolker HR, Banich MT (2015) Organization of the human frontal pole revealed by large-scale DTI-based connectivity: implications for control of behavior. PLoS One 10:e0124797.

Raud L, Westerhausen R, Dooley N, Huster RJ (2020) Differences in unity: the go/no-go and stop signal tasks rely on different mechanisms. Neuroimage 210:116582.

Rezvanfard M, Noroozi A, Golesorkhi M, Ghassemian E, Eghbali AN, Mokri A, Ekhtiari H (2017) Comparison of response inhibition behavior between methadone maintenance patients and active opiate users. Int J High Risk Behav Addict 6:e33257.

Ruxton GD (2006) The unequal variance t-test is an underused alternative to Student's *t*-test and the Mann–Whitney *U* test. Behavioral Ecology 17:688–690.

Sakai K, Passingham RE (2006) Prefrontal set activity predicts rule-specific neural processing during subsequent cognitive performance. J Neurosci 26:1211–1218.

Sheehan DV, Lecrubier Y, Sheehan KH, Amorim P, Janavs J, Weiller E, Hergueta T, Baker R, Dunbar GC (1998) The Mini-International Neuropsychiatric Interview (M.I.N.I.): the development and validation of a structured diagnostic psychiatric interview for DSM-IV and ICD-10. J Clin Psychiatry 59 Suppl 20:22–33.

Shi Z, Langleben DD, O'Brien CP, Childress AR, Wiers CE (2021) Multivariate pattern analysis links drug use severity to distributed cortical hypoactivity during emotional inhibitory control in opioid use disorder. Neuroimage Clin 32:102806.

Sjoerds Z, van den Brink W, Beekman ATF, Penninx BW, Veltman DJ (2014) Response inhibition in alcohol-dependent patients and patients with depression/anxiety: a functional magnetic resonance imaging study. Psychol Med 44:1713–1725.

Stanislaw H, Todorov N (1999) Calculation of signal detection theory measures. Behav Res Methods Instrum Comput 31:137–149.

Swick D, Ashley V, Turken AU (2008) Left inferior frontal gyrus is critical for response inhibition. BMC Neurosci 9:102.

Tanji J, Shima K (1994) Role for supplementary motor area cells in planning several movements ahead. Nature 371:413–416.

Tiffany ST, Singleton E, Haertzen CA, Henningfield JE (1993) The development of a cocaine craving questionnaire. Drug Alcohol Depend 34:19–28.

Tullett AM, Inzlicht M (2010) The voice of self-control: blocking the inner voice increases impulsive responding. Acta Psychol (Amst) 135:252–256.

Tustison NJ, Avants BB, Cook PA, Zheng Y, Egan A, Yushkevich PA, Gee JC (2010) N4ITK: improved N3 bias correction. IEEE Trans Med Imaging 29:1310–1320.

Verbruggen F, Logan GD (2008) Response inhibition in the stop-signal paradigm. Trends Cogn Sci 12:418–424.

Verbruggen F, Logan GD, Stevens MA (2008) STOP-IT: windows executable software for the stop-signal paradigm. Behav Res Methods 40:479–483.

Verbruggen F, et al. (2019) A consensus guide to capturing the ability to inhibit actions and impulsive behaviors in the stop-signal task. Elife 8: e46323.

Verdejo-García AJ, Perales JC, Pérez-García M (2007) Cognitive impulsivity in cocaine and heroin polysubstance abusers. Addict Behav 32:950–966.

Vossel S, Geng JJ, Fink GR (2014) Dorsal and ventral attention systems. Neuroscientist 20:150–159.

Wager TD, Nichols TE (2003) Optimization of experimental design in fMRI: a general framework using a genetic algorithm. Neuroimage 18:293–309.

Wang W, Worhunsky PD, Zhang S, Le TM, Potenza MN, Li C-SR (2018) Response inhibition and fronto-striatal-thalamic circuit dysfunction in cocaine addiction. Drug Alcohol Depend 192:137–145.

Woolrich MW, Ripley BD, Brady M, Smith SM (2001) Temporal autocorrelation in univariate linear modeling of FMRI data. Neuroimage 14:1370–1386.

Yang B, Yang S, Zhao L, Yin L, Liu X, An S (2009) Event-related potentials in a Go/Nogo task of abnormal response inhibition in heroin addicts. Sci China C Life Sci 52:780–788.

Zhang Y, Brady M, Smith S (2001) Segmentation of brain MR images through a hidden Markov random field model and the expectation-maximization algorithm. IEEE Trans Med Imaging 20:45–57.

Zhang Y, Zhang S, Ide JS, Hu S, Zhornitsky S, Wang W, Dong G, Tang X, Li C-SR (2018) Dynamic network dysfunction in cocaine dependence: graph theoretical metrics and stop signal reaction time. Neuroimage Clin 18:793–801.

Zilverstand A, Huang AS, Alia-Klein N, Goldstein RZ (2018) Neuroimaging impaired response inhibition and salience attribution in human drug addiction: a systematic review. Neuron 98:886–903.